Biosensors and Bioelectronics 85 (2016) 649–656

Contents lists available at ScienceDirect

Biosensors and Bioelectronics

journal homepage: www.elsevier.com/locate/bios

A microfluidic biosensor using graphene oxide and aptamer-functionalized quantum dots for peanut allergen detection

Xuan Weng, Suresh Neethirajan*

BioNano Laboratory, School of Engineering, University of Guelph, Guelph, Canada N1G 2W1

ARTICLE INFO

Article history:
Received 7 May 2016
Received in revised form
20 May 2016
Accepted 22 May 2016
Available online 24 May 2016

Keywords:
Aptamer
Graphene oxide
Quantum dots
Ara h 1
Microfluidics

ABSTRACT

The increasing prevalence of food allergies and the intake of packing foods in the past two decades urge the need for more rapid, accurate, and sensitive assays to detect potential allergens in food in order to control the allergen content. Most of the commercial analytical tools for allergen detection rely on immunoassays such as ELISA. As far as disadvantages, ELISA can be time-consuming and expensive. Biosensors appear as a suitable alternative for the detection of allergens because they are rapid, highly sensitive, selective, less expensive, environmentally friendly, and easy to handle. In this study, we developed a microfluidic system integrated with a quantum dots (Qdots) aptamer functionalized graphene oxide (GO) nano-biosensor for simple, rapid, and sensitive food allergen detection. The biosensor utilized Qdots-aptamer-GO complexes as probes to undergo conformational change upon interaction with the food allergens, resulting in fluorescence changes due to the fluorescence quenching and recovering properties of GO by adsorption and desorption of aptamer-conjugated Qdots. This one-step 'turn on' homogenous assay in a ready-to-use microfluidic chip took ~10 min to achieve a quantitative detection of Ara h 1, one of the major allergens appearing in peanuts. The results suggested this system had remarkable sensitivity and selectivity. The integration of a microfluidics platform in a homemade miniaturized optical analyzer provides a promising way for the rapid, cost-effective, and accurate on-site determination of food allergens. This biosensor can also be extended to the detection of other food allergens with a selection of corresponding aptamers.

1. Introduction

Food allergies have become an increasing food safety and public health concern throughout the world due to their significant effect on people's morbidity and their cost for medical visits and treatments. For allergic individuals, avoidance of the food is the only way to protect themselves against a food allergy reaction as there is no cure for food allergies (Alves et al., 2015). Although the intended presence or absence of allergens can be read from the food labels from manufacturers, undeclared allergenic substances can be inadvertently introduced into a food by uncontrolled cross-contamination, the improper use of rework, or labelling errors and cause an accidental exposure. The peanut allergy is one of the leading causes of severe food-induced allergic reactions due to its persistency and life-threatening nature. Unlike other allergies, the peanut allergy tends to be lifelong with a high risk of accidental exposure, and in highly sensitized people, trace amounts may induce an allergic reaction (Al-Muhsen et al., 2003). Among the allergenic proteins of peanuts, Ara h 1, a homotrimeric protein with a molecular weight of 65 kDa, is identified as one of the major peanut allergens presenting in a wide variety of peanuts or peanut products and shown to account for almost 95% of all peanut-allergenicity reactions (Peeters et al., 2014; Burks et al., 1991; Koppelman et al., 2004). Monitoring the presence or cross-contamination of peanut proteins is extremely important to both the food industry and sensitive individuals. With the increase in allergen awareness and regulations, many analytical methods have been developed: immunochemical methods such as ELISA (Pomés et al., 2003; Peng et al., 2013), lateral flow assay (Wang et al., 2015), DNA-based methods such as PCR (Zhang et al., 2015), and mass spectrometry (Monaci et al., 2015). Usually, these methods rely on either monoclonal or polyclonal antibodies, which are expensive to produce and possess a limited working range and shelf life (Peeters et al., 2014; Gutteridge and Thornton, 2005; Amaya-González et al., 2013; van Hengel, 2007), and the occurrence of cross-reactions is frequent. In contrast, aptamers, single-stranded oligonucleotide, or peptide sequences selected through the systematic evolution of ligands by exponential enrichment (SELEX) exhibit high affinity and specificity to various classes of target molecules. As an alternative to natural antibodies, aptamers

* Corresponding author.
E-mail address: sneethir@uoguelph.ca (S. Neethirajan).

http://dx.doi.org/10.1016/j.bios.2016.05.072
0956-5663/

are less expensive but more stable while still having a similar affinity to their target molecules. In addition, the synthesis and modification of aptamers are relatively easy (Zuo et al., 2013). Recently, aptamers have also been synthesized for food allergens detection (Tran et al., 2013, 2010; Nadal et al., 2013; Mairal et al., 2014; Amaya-González et al., 2014).

Biosensors have presented the potential for real-time, direct monitoring of allergens due to their high sensitivity and selectivity while remaining relatively inexpensive, environmentally friendly, and rapid (Alves et al., 2015). However, information on the development of aptamer-based biosensors for food allergen analysis is scarcely available in the literature as it is a recent growth area. As mentioned above, aptamers have emerged as effective molecular recognition elements for ligand analysis in biosensors due to the easy modification and control without obvious deactivation. The fluorescently labeled aptamers can be used in optical sensors for molecular recognition (Cui et al., 2011).

The unique properties of nanomaterials offer excellent prospects toward the development of novel molecular diagnostic tools (He et al., 2010). Graphene oxide (GO), a single-atom-thick two-dimensional (2D) carbon nano-material, has received extensive interest in numerous biosensor applications because of its unique optical, electronic, thermal, and long-lasting biocompatibility properties (Song et al., 2013). More importantly, GO can be an efficient quencher for various fluorophores (Huang and Liu, 2012) due to the non-radioactive electronic excitation energy transfer between the fluorophore and GO (Swathi and Sebastian, 2009) and its large absorption cross section (Geim and Novoselov, 2007), providing very high quenching efficiency. In addition, GO was found to be able to interact with amino acids, peptide, and proteins by fluorescence quenching (Li et al., 2012). With its superior fluorescence quenching and adsorption capacity, GO has been increasingly used for making FÖrster resonance energy transfer (FRET) biosensors, aptasensors, drug-delivery vehicles, and imaging agents (Huang and Liu, 2012; Lu et al., 2015; Wang et al., 2010; Morales-Narváez et al., 2012; Zhang et al., 2011; Lu et al., 2009). Quantum dots (Qdots) are nanomaterials that have also been increasingly used in immunoassays, fluorescent biosensing, and imaging applications (Bogomolova and Aldissi, 2011; Algar et al., 2010; Frasco and Chaniotakis, 2010) due to the chemical stability, efficient and stable fluorescence signals, and superior biological probes compared with traditional organic dyes. Aptamer conjugated Qdots for bio-recognition have been performed since 2005 (Levy et al., 2005) and later were used in the detection of protein, small biomolecules, and food-borne pathogens (Bogomolova and Aldissi, 2011). Strategies based on FRET have attracted more attention due to their inherently high sensitivity (Abachi and Noureini, 2011; He et al., 2012) and homogeneous detections (Zeng et al., 2012).

In our study, we integrated an aptamer/Qdots-functionalized graphene oxide (GO) biosensor for food allergen detection on a microfluidic platform based on the fluorescence quenching and recovering properties of GO through the adsorption and desorption of QDots-conjugated aptamers. We successfully detected the major peanut allergen Ara h1 with a high sensitivity and selectivity by using this biosensor. In addition to the decreased sample/reagent consumption and rapidity introduced by using microfluidics, this homogenous assay does not require complicated probe immobilization or tedious procedures. The fluorescence signals were measured on a miniaturized optical detector, which facilitated the portability of the whole system.

2. Materials and method

The Ara h 1 aptamer synthesis was obtained from IDT technologies (Coralville, Iowa, USA) and had the following 80 base pairs sequence:

5′ TCGCACATTCCGCTTCTACCGGGGGGGTCGAGCGAGTGAGCGAA TCTGTGGGTGGGCCGTAAGTCCGTGTGTG CGAA 3′.

The 5′ end was modified with biotin. Ara h 1, Ara h 2, and Ara h 3 standards and the Ara h 1 ELISA kit were purchased from INDOOR Biotechnologies Inc. (Charlottesville, VA, USA). Commercially available CdSe Qdots modified with covalently attached streptavidin (Qdot® 545 ITK™ Streptavidin Conjugates) were purchased from Invitrogen Life Technologies (Burlington, ON, Canada). Polydimethylsiloxane (PDMS, Sylgard, 184) was obtained from Dow Corning (Midland, MI, USA). Graphene oxide, phosphate-buffered saline (PBS), and all other mentioned chemicals and solvents were purchased from Sigma-Aldrich (Oakville, ON, Canada). Unless otherwise noted, all solutions were prepared with ultrapure DI water.

2.1. Preparation of aptamer-conjugated quantum dots

The dried aptamer pellet was firstly resuspended in TE buffer (10 mM Tris–HCl, 0.1 mM EDTA, pH 8.0) to achieve a 100 μM concentration. The resuspended aptamer was incubated at room temperature for 30 min, created aliquots, and stored at −20 °C. Prior to use, the aptamer was diluted to the working concentration in the folding buffer (1 mM $MgCl_2$, 1 × PBS, pH 7.4) and heated at 85 °C for 5 min. The cooling-down dilutions were ready for use.

Streptavidin-conjugated quantum dots of 2 μM were mixed with 3.2 μM 5′-biotin aptamers in a 200 μL PBS (pH 7.4, 0.01 M). The quantum dots were covalently linked to 5′-biotin aptamers via streptavidin-biotin interaction. The mixture was incubated under gentle mixing at room temperature. After incubation, the Qdots-aptamer conjugates mixture was subjected to ultrafiltration with PBS (three times, 15 min at 6000 rpm, cut-off filter 50 kD) to remove the excess of the unbound aptamer. The conjugates were finally resuspended in a 0.01 M PBS solution (pH 7.4) for Ara h 1 detection.

2.2. Preparation of Qdots-aptamer-GO quenching system

GO was diluted in ultrapure DI water and mixed with the Qdots-aptamer conjugates solution. The excellent dispersibility is very critical for its sufficient interaction with aptamer molecules. The BSA solution was added into the mixture at a final concentration of 0.5%. The mixture of Qdots-aptamer conjugates and GO was incubated for a period of time to quench the fluorescence of the Qdots-aptamer conjugates. Optimal GO concentration and quenching time were investigated.

2.3. Detection of Ara h 1

Different concentrations of Ara h 1 standard solution or food samples were added into the Qdots-aptamer-GO quenching system with gentle shaking. The mixtures were then incubated at room temperature. Incubation times of 5, 10, 15, and 20 min were investigated. Fluorescence spectra of the mixtures were measured to evaluate the Qdots fluorescence recovery and make the standard curve. The schematic of the sensing mechanism is shown in Fig. 1A. Fluorescence of Qdots is quenched via FRET process between the Qdots-aptamer probes and GO due to their self-assembly through specific π–π interaction. In the presence of the target Ara h 1 protein, the association constant between the Qdots-aptamer probes and Ara h1 is bigger than that between the Qdots-aptamer probes and GO, resulting in the release of the Qdots-aptamer probes from GO and thus the recovery of the fluorescence of Qdots.

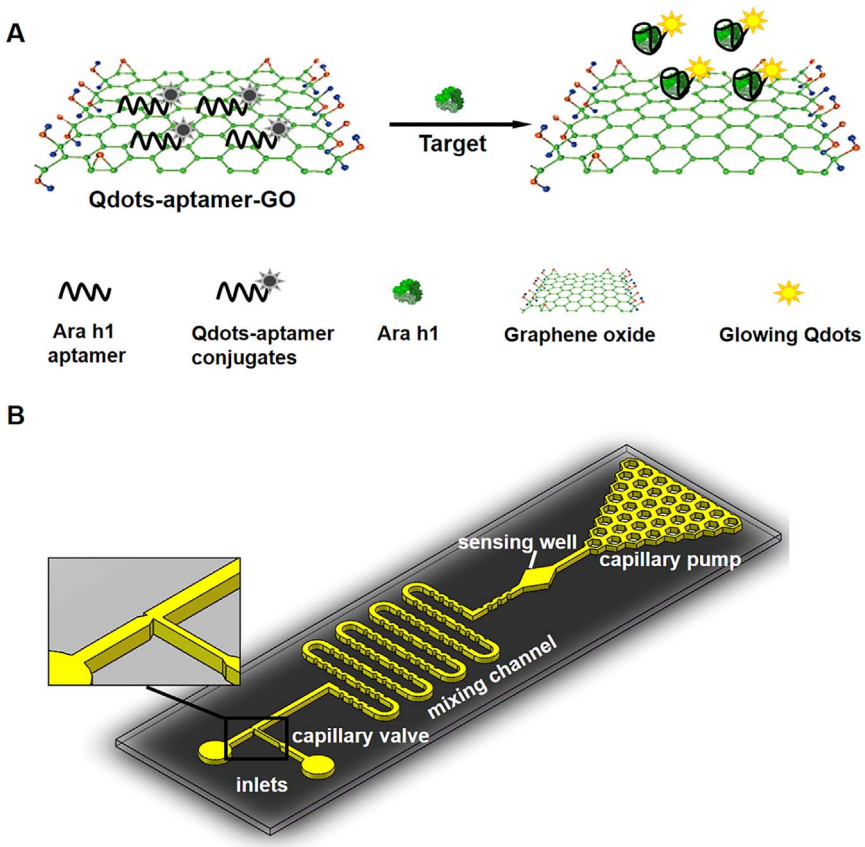

Fig. 1. (A) Schematic of the sensing mechanism of the Qdots-aptamer-GO quenching system. (B) Schematic diagram of microfluidic chip design (not to scale). The microfluidic chip had two inlets for loading the Qdots-aptamer-GO probe mixture and the Ara h 1 sample, respectively. The main channel of 200 μm wide and 60 μm deep consisted of a mixing/incubation channel, a sensing well, and a capillary pump at the end. The long and zigzag-shaped channel was designed to enhance the mixing effect. The "diamond"-shaped well was the sensing well aligned to the sensing window of the Si photodiode. The flow was driven by the capillary forces.

2.4. Characterization of the Qdots-aptamer probes

The modification of the fluorescent Qdots and Ara h 1 aptamers were bridged with a streptavidin-biotin site-specific bioconjugation system via the extraordinarily high affinity of streptavidin homo-tetramers for biotin. Then, the Qdots-aptamer probes were characterized by fluorescence spectra (Synergy H4 Hybrid Multi-Mode Microplate Reader, Biotek, Winooski, VT, USA), TEM (Tecnai G2 F20, FEI, Hillsboro, Oregon, USA), and a DLS system (ZetaPlus Zeta potential analyzer, Brookhaven Instruments Corporation, Holtsville, NY, USA).

2.5. Optimization

Optimization was firstly performed by investigating the molar ratio (1:1, 1:4, and 1:8) of between Qdots and Ara h 1 aptamer and incubation time (30 min, 4 h, and 12 h) during the Qdots modification. In the sensing processing, concentrations of graphene oxide and the incubation times for quenching and recovery affect not only the quenching rate but also the recovery efficiency, which can directly affect the detection sensitivity. Hence, the optimization of GO concentration (0–0.1 mg/mL) and quenching/recovery time (0–15 min) were also investigated.

2.6. Microplate reader and fluorescence microscopic detection

To validate the performance of the Qdot-aptamer-GO quenching system, fluorescence analysis was conducted by fluorescent spectra analysis on a microplate reader (Synergy H4 Hybrid Multi-Mode Microplate Reader, Biotek, Winooski, VT, USA) and fluorescent imaging on a fluorescent microscopy (Nikon Eclipse Ti, Nikon Canada Inc., Mississauga, ON, Canada).

2.7. Microfluidic biochip fabrication and signal capture

The schematic design of the microfluidic biochip is shown in Fig. 1B. The microfluidic chip consisted of two inlets, a mixing/incubation channel, a sensing well, and a capillary pump. The powerless sampling can be generated by this "hexagons" capillary pump by splitting the capillary pump into hundreds of smaller parallel microchannels; hence, the liquid could be sucked into the microfluidic channel by the capillary force. The design at the entrance of the mixing/incubation channel was a capillary-driven retarding valve (Mohammed and Desmulliez, 2013), which helped to avoid air capture in the microchannel when dispensing the Qdots-aptamer-GO probe mixture and the Ara h 1 sample into the inlets. In addition, to enhance the mixing effect of the mixture in the microchannel, a zigzag microchannel was designed. The total length of the mixing microchannel was around 10 cm.

The microfluidic chips were fabricated by using the standard soft lithography technique. A master-carrying microchannel mold was firstly prepared by spin-coating a thin film of SU-8 negative photoresist (MicroChem, Westborough, MA, USA) on a silicon wafer followed by pre-baking. The photoresist film covered with a mask bearing the desired microchannel geometry was then exposed to UV light. After post-baking and developing, a master mold could be obtained. The second step was making the PDMS chips. A degassed mixture of PDMS prepolymer and curing agent (10:1, w/w) was poured over the master mold and cured at 75 °C for about 4 h. After the incubation, the PDMS replica was peeled

off the master mold, and the inlets were punched. The PDMS microchannel was placed on a glass slide filled with 10 mg/mL BSA solution and left to dry at room temperature, which was performed to prevent the non-specific adsorption of the desired proteins onto the channel wall. Then, the PDMS microchannel was peeled away from the slide and sealed against a clean glass slide after the oxygen plasma was treated for 40 s.

To make the whole sensing system capable of on-site detection, the fluorescence signals were measured by a miniaturized optical detector. The details of the optical detector can be found in our previous study (Weng et al., 2015). Briefly, the miniaturized optical detector consisted of LED (447.5 nm, Luxeon Rebel, Luxeon Star LEDs, Brantford, ON, Canada) mounted on the top to provide excitation light and a low-noise, high-sensitivity Si photodiode (Hamamatsu, Bridgewater, NJ, USA) mounted on the bottom for emission light capture. The PDMS well was placed in between and aligned to both the LED and the sensing window of the photodiode. Excitation (445/20–25 nm, Semrock, Rochester, NY, USA) and emission (531/20–25 nm, Semrock, Rochester, NY, USA) optical filters were used to reduce interference. All components were assembled in a container ($10 \times 6 \times 5$ cm^3) to block ambient light. The collected light intensity signal by the Si photodiode was then digitized and transferred to a PC for storage and analysis by a programmable microcontroller (Arduino Uno, SparkFun Electronics, Niwot, CO, USA).

Based on the optimization, 10 μL of Qdots-aptamer probes with a GO solution with a final concentration at 0.05 mg/mL and 10 μL of Ara h 1 standard solution and the food sample solution were added in the inlets of the microfluidic device, respectively. The fluorescence intensity was measured immediately when the mixture flew into the sensing well as a reference by the photodiode. After 5 min of recovery, the fluorescence intensity was measured and recorded again, and the difference was used to differentiate the Ara h 1 concentration.

3. Results and discussion

3.1. Characterization of the Qdots-aptamer probes

Conjugation may cause a change in the nanoparticle size, zeta potential, and so on. Hence, the Qdots-aptamer probes were characterized first. The morphology of the Qdots before and after conjugation with the aptamer were characterized by TEM imaging as shown in Fig. 2A and B. Both nanoparticles showed a cone-like shape and were well dispersed, but no significant changes were observed in the particle size (~10 nm) of Qdots-aptamer probes. The hydration diameters of the Qdots before and after conjugation were measured and compared by dynamic light scattering (DLS) analysis. As shown in Fig. 2C, the mean hydration diameter of the

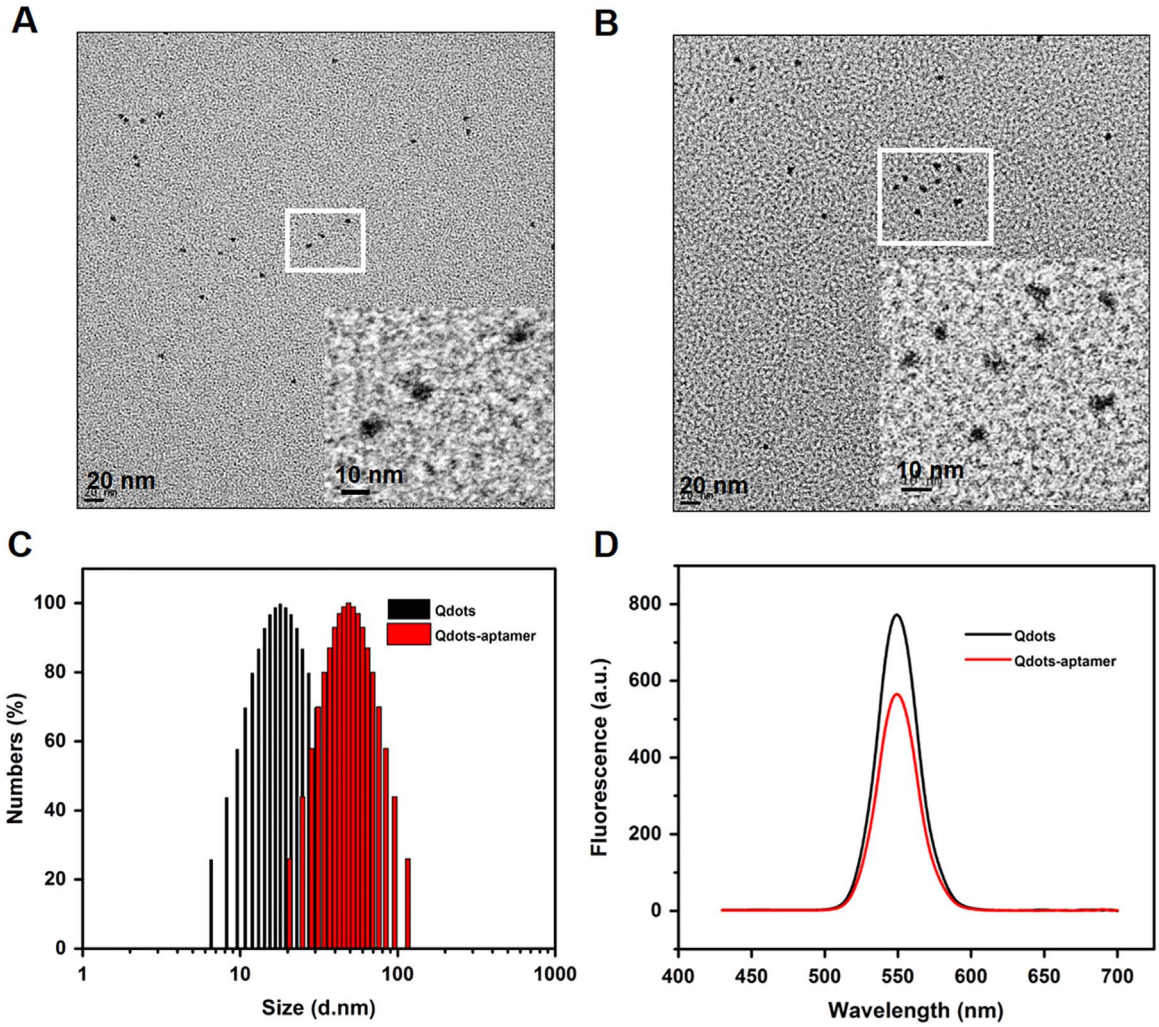

Fig. 2. Characterization of Qdots-aptamer probes. (A) TEM images of Qdots-streptavidin conjugates; (B) TEM images of Qdots-aptamer probes. (C) Particle size distribution of Qdots-streptavidin conjugates and Qdots-aptamer probes by DLS. The mean hydration diameter of the QDs and QDs-aptamer are 21.9 nm and 47.9 nm, respectively. (D) Fluorescence spectra of Qdots and Qdots-aptamer probes.

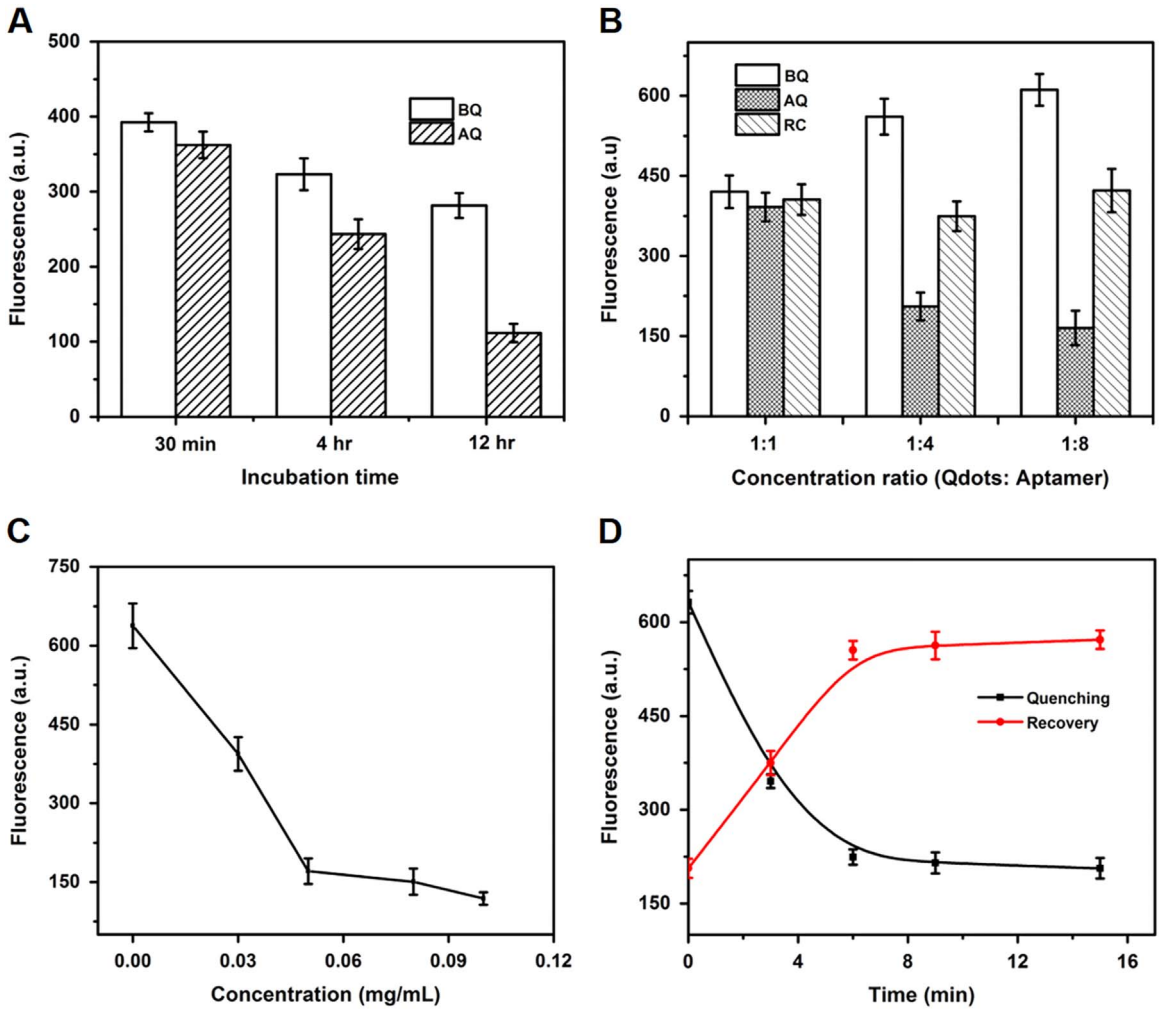

Fig. 3. Optimization of (A) incubation time of Qdots conjugation with Ara h 1 aptamer; (B) aptamer concentrations in effecting quenching and recovery performance; (C) GO concentrations in effecting quenching and recovery performance; (D) quenching and recovery time.

nanoparticle increased from 21.9 nm and 47.9 nm while the zeta (ξ) potential values increased from -34.3 ± 3.0 mV to -42.2 ± 4.1 mV. Since the modifier streptavidin and Ara h 1 aptamer could not be observed by TEM, the particle sizes detected by TEM were smaller than those detected by DLS. In addition, a decrease of the fluorescence intensity of the Qdots before and after conjugation was also observed (Fig. 2D). The concentration of Qdots in both solutions was 0.2 μM. These results indicated that Qdots were successfully bound with Ara h1 aptamers.

3.2. Optimization and sensing mechanism validation

The preparation of the Qdots-aptamer probes was the key for the sensing event, which significantly affected the fluorescence quenching and recovery; hence, the conjugation of Ara h 1 aptamer onto the Qdots was studied. The incubation time and aptamer concentration were optimized. 30 min, 4 h, and 12 h of incubation were tested, and the fluorescence response before quenching (BQ) and after quenching (AQ) were investigated as shown in Fig. 3A. The overnight incubated probes presented a significant quenching effect compared to the other two. Three different ratios of concentration, 1:1, 1:4, and 1:8, between Qdots and Ara h 1 aptamers were tested by observing the fluorescence intensities before quenching (BQ), after quenching (AQ), and after recovery (RC). The result of detection of Ara h1 of 2000 ng/mL was shown in Fig. 3B. After the addition of graphene oxide of the same concentration, fluorescence quenching occurred for all the three concentrations. However, low-quenched fluorescence and high-recovered fluorescence would provide high sensitivity. From the result, we see that the higher ratio of 1:8 presented lower and higher fluorescence in quenching and recovery. In addition, we found that when the concentration ratio was bigger than 1:8, no significant improvement was found. Therefore, the ratio of 1:8 and overnight incubation were used in the following tests. To obtain the optimized quenching effect, the concentrations of GO were also investigated. As shown in Fig. 3C, bigger fluorescence quenching occurred with the increasing of the concentration of GO ranging from 0.03 mg/mL to 0.1 mg/mL. From the result, 0.05 mg/mL presented the superior quenching effect, while a concentration higher than 0.05 mg/mL did not show a significant difference. However, a distinctive lower fluorescence intensity was observed at the concentration of 0.1 mg/mL, which may be caused by the turbidity due to the high concentration of GO. Hence, a final concentration of 0.05 mg/mL of GO in the mixture was used. The assay time depended on the quenching and recovery time; hence, the incubation times for fluorescence quenching and recovery were investigated, the result of which was shown in Fig. 3D. Fluorescence intensities in the processes of quenching and recovery were measured at the time points at 0, 3, 6, 9, and 15 min, respectively. We found that the significant changes of quenching and recovery occurred within the first 6 min of the both processes; hence, 5 min was used as the quenching and recovery time. Therefore, 10 min

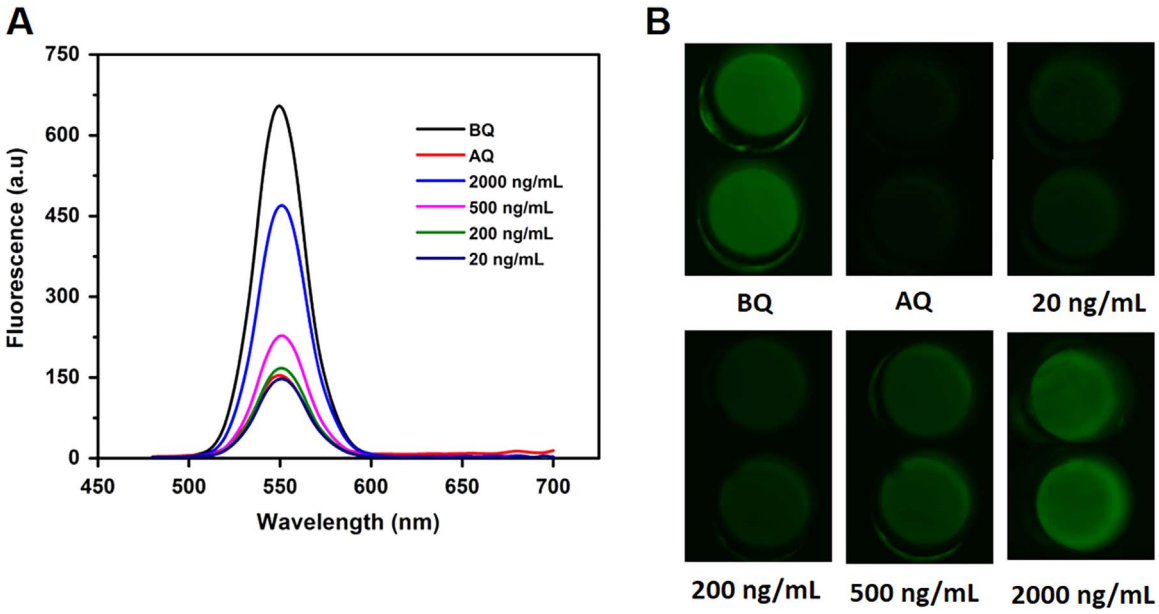

Fig. 4. Fluorescence spectra (A) and fluorescence images (B) of Ara h1 standard solution of various concentrations by Qdots-aptamer-GO system before quenching (BQ), after quenching (AQ), and recovery.

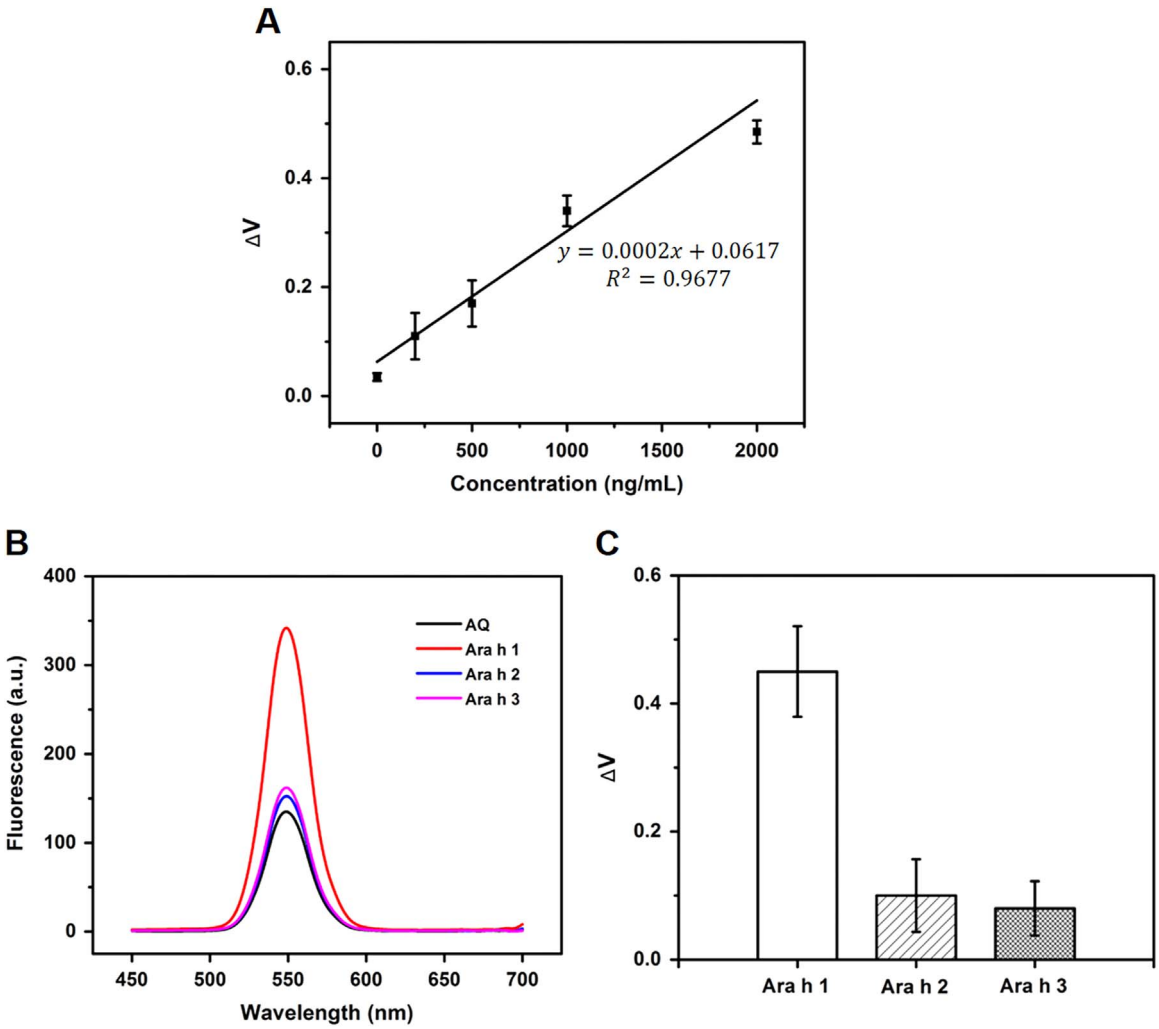

Fig. 5. (A) Standard calibration curve for the relative voltage output change depending on fluorescence intensity caused by Ara h 1 concentration ranging from 200 to 2000 ng/mL. Each data point was obtained from three independent measurements. (B) Fluorescence spectra and (C) relative voltage output difference depending on fluorescence intensity in the presence of Ara h 1, Ara h 2, and Ara h 3 of 1000 ng/mL, respectively.

Table 1
Determination of Ara h 1 concentration in actual samples by our biosensor and an ELISA kit.

Spiked concentration (ng/mL)	Measured by biosensor (ng/mL) (%)	Recovery by biosensor (%)	Measured by ELISA kit (ng/mL) (%)	Recovery by ELISA kit (%)
0	116.5 ± 3.5		97.4 ± 3.4	
200	291.5 ± 5.6	87.5	269.1 ± 4.0	85.8
500	566.5 ± 4.9	90	590.7 ± 5.5	98.7
1000	1041.5 ± 4.2	92.5	1001.3 ± 3.5	90.4

was considered the total assay time for a single test.

With the optimized settings obtained above, full assays on various concentrations of Ara h 1 standard solution ranging from 20 ng/mL to 2000 ng/mL were conducted in a 384 microplate well and read by a microplate reader to validate the sensing mechanism. The fluorescence spectra and fluorescence images were shown in Fig. 4A and B.

3.3. Detection by optical detector

The time-dependent fluorescence changes upon the reaction of Qdots-aptamer-GO with Ara h 1 standard solution were investigated by a custom-designed miniaturized optical detector, which is shown in Fig. 5A. Based on the optimization results, 5 min was taken as the quenching time and fluorescence recovery time. To minimize the error, the output of the photodiode after quenching and recovery were recorded, and the relative difference between these two value was used to differentiate the sample concentration. As shown in Fig. 5A, the output of the photodiode increased as the concentration of Ara h 1 increased, which indicates the recovered fluorescence intensity of the Qdots was intensified. The relative differences obtained by detecting Ara h 1 standard solution of various concentrations were used to make the standard curve. An R^2 value of 0.9677 was found for the linear response region between 200 ng/mL and 2000 ng/mL with detection limits of 56 ng/mL (Thomsen et al., 2003).

3.4. Specificity and food sample detection

Ara h 1, Ara h 2, and Ara h 3 are all the major allergens presented in peanuts. Specificity analysis was performed by an investigation of the system response to the possible interferences introduced by Ara h 2 and Ara h 3. Ara h 1, Ara h 2, and Ara h 3 of the same concentration at 1000 ng/mL were assayed by the Qdots-aptamer-GO system. As shown in Fig. 5B and C, little fluorescence recovery was found by Ara h 2 and Ara h 3 compared to the significant fluorescence intensity increase by Ara h 1, which demonstrated the high selectivity and specificity of our system in determining Ara h 1.

To validate the performance of our optical biosensor, when working on the real food sample was assayed, Ara h 1 in a biscuit was detected by our method and a commercial ELISA kit for a comparison. Food sample preparation was conducted by following the procedure indicated in the manual of the commercial kit. Briefly, 1 g of the homogenized biscuit sample was mixed with 20 mL of the sample extraction solution provided by the kit and followed by incubation in a water bath at 60 °C for 15 min After being cooled down under room temperature, the solution mixture was centrifuged at 2000 × *g* for 10 min The supernatant of the mixture was filtered through a filter syringe (GHP Membrane Disc Filters, VWR International; Suwanee, GA, USA) with 0.2 μm diameter pores and made a series of dilutions for detection. The precision of this method in terms of recovery rate was evaluated by spiking Ara h 1 standard solutions of 200, 500, and 1000 ng/mL into the food samples. Each concentration was performed three times to ensure the consistency of the response trend, and the recovery rate was calculated as follows:

$$Recovery\,(\%)=\frac{\bar{C}'-\bar{C}_0}{C_S}$$

where $\bar{C}'$ is the mean Ara h 1 concentration of the spiked samples, $\bar{C}_0$ is the mean Ara h 1 concentration of the blank sample, and C_S is the concentration of the standard solution spiked into the sample.

The results in Table 1 show that the spiked recoveries measured by the presented biosensor were consistent with the ELISA kit.

4. Conclusions

A microfluidic biosensor for Ara h 1 detection was developed by using a quencher system with graphene oxide and aptamer-functionalized quantum dots. This fluorescence was “turned off” by a fluorescence resonance energy transfer between the Qdots-aptamer and graphene oxide and “turned on” with the addition of Ara h 1 due to the better association constant between the Qdots-aptamer and Ara h1 compared to that between the Qdots-aptamer and GO, which led to the release of the Qdots-aptamer from GO, resulting in the recovery of the fluorescence of Qdots. The Qdots-aptamer probes showed superior fluorescent properties. Based on the principle above, an assay for Ara h1 detection was performed on a microfluidic platform with a miniaturized optical sensor. The results proved that the presented method was capable of the simple, rapid, sensitive, and reliable detection of Ara h 1 with a detection limit of 56 ng/mL. The results also suggested this method had the potential for on-site determination for rapidly detecting food allergens with the flexibility to select aptamers for specifically targeted allergens.

Acknowledgements

The authors sincerely thank the Natural Sciences and Engineering Research Council of Canada (400929) and the Canada Foundation for Innovation (500512) for funding this study.

References

Abachi, F., Noureini, S.K., 2011. Clin. Biochem. 44, S257.
Algar, W.R., Tavares, A.J., Krull, U.J., 2010. Anal. Chim. Acta 673 (1), 1–25.
Alves, R.C., Barroso, M.F., González-García, M.B., Oliveira, M.B.P.P., Delerue-Matos, M.C., 2015. New trends in food allergens detection: towards biosensing strategies. Crit. Rev. Food Sci. Nutr. http://dx.doi.org/10.1080/10408398.2013.831026.
Al-Muhsen, S., Clarke, A.E., Kagan, R.S., 2003. Can. Med. Am. J. 168 (10), 1279–1285.
Amaya-González, S., de-los-Santos-Álvarez, N., Miranda-Ordieres, A.J., Lobo-Castañón, M.J., 2013. Sensors 13 (12), 16292–16311.
Amaya-González, S., de-los-Santos-Álvarez, N., Miranda-Ordieres, A.J., Lobo-Castañón, M.J., 2014. Anal. Chem. 86 (5), 2733–2739.
Burks, A.W., Williams, L.W., Helm, R.M., Connaughton, C., Cockrell, G., O'Brien, T., 1991. J. Allergy Clin. Immunol. 88 (2), 172–179.
Bogomolova, A., Aldissi, M., 2011. Biosens. Bioelectron. 26 (10), 4099–4103.
Cui, Z.Q., Ren, Q., Wei, H.P., Chen, Z., Deng, J.Y., Zhang, Z.P., Zhang, X.E., 2011. Nanoscale 3 (6), 2454–2457.
Frasco, M.F., Chaniotakis, N., 2010. Anal. Bioanal. Chem. 396 (1), 229–240.
Geim, A.K., Novoselov, K.S., 2007. Nat. Mater. 6 (3), 183–191.
Gutteridge, A., Thornton, J.M., 2005. Trends Biochem. Sci. 30, 622–629.
He, S.J., Song, B., Li, D., Zhu, C.F., Qi, W.P., Wen, Y.Q., Wang, L.H., Song, S.P., Fang, H.P., Fan, C.H., 2010. Adv. Funct. Mater. 20, 453–459.
He, Y., Lu, M., Cao, J., Lu, H.P., 2012. ACS Nano 6, 1221–1229.
Huang, P.J.J., Liu, J., 2012. Small 8 (7), 977–983.
Koppelman, S.J., Wensing, M., Ertmann, M., Knulst, A.C., Knol, E.F., 2004. Clin. Exp. Allergy 34, 583–590.
Levy, M., Cater, S.F., Ellington, A.D., 2005. Chem. Bio. Chem. 6 (12), 2163–2166.
Li, S., Aphale, A.N., Macwan, I.G., Patra, P.K., Gonzalez, W.G., Miksovska, J., Leblanc, R. M., 2012. ACS Appl. Mater. Interfaces 4 (12), 7069–7075.

Lu, C.H., Yang, H.H., Zhu, C.L., Chen, X., Chen, G.N., 2009. Angew. Chem. 121 (26), 4879–4881.
Lu, Z., Chen, X., Wang, Y., Zheng, X., Li, C.M., 2015. Microchim. Acta 182 (3–4), 571–578.
Mairal, T., Nadal, P., Svobodova, M., O'Sullivan, C.K., 2014. Biosens. Bioelectron. 54, 207–210.
Mohammed, M.I., Desmulliez, M.P.Y., 2013. Microsyst. Technol. 19 (6), 809–818.
Monaci, L., De Angelis, E., Bavaro, S.L., Pilolli, R., 2015. Food Addit. Contam. Part A 32 (10), 1607–1616.
Morales-Narváez, E., Pérez-López, B., Pires, L.B., Merkoçi, A., 2012. Carbon 50 (8), 2987–2993.
Nadal, P., Svobodova, M., Mairal, T., O'Sullivan, C.K., 2013. Anal. Bioanal. Chem. 405 (29), 9343–9349.
Peeters, M., Jiménez-Monroy, K.L., Libert, C., Eurlings, Y., Cuypers, W., Wackers, G., Duchateau, S., Robaeys, P., Nesládek, M., van Grinsven, B., Pérez-Ruiz, E., Lammertyn, J., Losada-Pérez, P., Wagner, P., 2014. J. Biosens. Bioelectron. 5, 155.
Peng, J., Song, S., Xu, L., Ma, W., Liu, L., Kuang, H., Xu, C., 2013. Int. J. Environ. Res. Public Health 10 (7), 2897–2905.
Pomés, A., Helm, R.M., Bannon, G.A., Burks, A.W., Tsay, A., Chapman, M.D., 2003. J. Allergy Clin. Immunol. 111 (3), 640–645.
van Hengel, A.J., 2007. Anal. Bioanal. Chem. 389 (1), 111–118.
Swathi, R.S., Sebastian, K.L., 2009. J. Chem. Phys. 130 (8), 086101.
Song, E., Cheng, D., Song, Y., Jiang, M., Yu, J., Wang, Y., 2013. Biosens. Bioelectron. 47, 445–450.
Thomsen, V., Schatzlein, D., Mercuro, D., 2003. Spectroscopy 18 (12), 112–114.
Tran, D.T., Knez, K., Janssen, K.P., Pollet, J., Spasic, D., Lammertyn, J., 2013. Biosens. Bioelectron. 43, 245–251.
Tran, D.T., Janssen, K.P., Pollet, J., Lammertyn, E., Anné, J., Van Schepdael, A., Lammertyn, J., 2010. Molecules 15 (3), 1127–1140.
Wang, Y., Deng, R., Zhang, G., Li, Q., Yang, J., Sun, Y., Li, Z., Hu, X., 2015. J. Agric. Food Chem. 63 (8), 2172–2178.
Wang, Y., Li, Z., Hu, D., Lin, C.T., Li, J., Lin, Y., 2010. J. Am. Chem. Soc. 132 (27), 9274–9276.
Weng, X., Zhao, W., Neethirajan, S., Duffield, T., 2015. J. Nanobiotechnol. 13 (1), 13.
Zeng, Q., Zhang, Y., Liu, X., Tu, L., Kong, X., Zhang, H., 2012. Chem. Commun. 48, 1781–1783.
Zhang, M., Yin, B.C., Tan, W., Ye, B.C., 2011. Biosens. Bioelectron. 26 (7), 3260–3265.
Zhang, W.J., Cai, Q., Guan, X., Chen, Q., 2015. Food Chem. 174, 547–552.
Zuo, P., Li, X., Dominguez, D.C., Ye, B.C., 2013. Lab Chip 13 (19), 3921–3928.